International Journal of Environmental Science and Technology (2024) 21:2881–2896
https://doi.org/10.1007/s13762-023-05160-9

ORIGINAL PAPER

Pre-concentration of pesticides in water using isophorone diamine multiwalled carbon nanotubes-based solid-phase extraction technique and analysis by gas chromatography–mass spectrometry

L. S. Sethoga[1,2] · T. Magadzu[1] · A. A. Ambushe[3]

Received: 25 February 2022 / Revised: 7 July 2023 / Accepted: 8 August 2023 / Published online: 19 September 2023

Abstract

The existence of pesticides in water at ultra-trace levels necessitates the use of a suitable pre-concentration method for their detection. The objective of this study was to develop an ultra-synthetic adsorbent to extract chlorpyrifos (CPF) and imazalil (IMA) pesticides in water. X-ray diffraction (XRD), thermogravimetric analysis (TGA) and Fourier transform infrared (FTIR) spectroscopy confirm that both oxidised and isophorone diamine multiwalled carbon nanotubes (IPD-MWCNTs) were successfully prepared with an intact structure; which was further confirmed by transmission electron microscopy (TEM) and energy-dispersive spectroscopy (EDS). The Brunauer–Emmet–Teller (BET) showed a high surface area of both oxidised and IPD-MWCNTs, which is linked to the formation of additional active sites. TGA further showed that the nanocomposites were highly stable within the pesticides quantification operating temperature. CPF and IMA were recovered using a low dosage of IPD-MWCNTs adsorbent (0.030 g) and eluted by a combined solvent (ethanol and chloroform (50:50, v/v)). The adsorbent was reusable over seven repeated cycles, with an acceptable percentage relative standard deviation (%RSD) ranging from 3 to 8%. The IPD-MWCNTs adsorption sites are highly stable and cannot be easily fouled, as compared to that of oxidised MWCNTs. Lower limits of detection (LOD) and quantification (LOQ) for CPF (0.026 and 0.078 $\mu g.L^{-1}$) and IMA (0.033 and 0.100 $\mu g.L^{-1}$) were achieved. Better recoveries for both analytes at low and high concentrations (as well as in real water samples) were obtained by IPD-MWCNTs whereas a conventional adsorbent (i.e. polymeric reverse phase) can only achieve better recoveries at high concentrations.

Keywords Adsorbent · Multiwalled carbon nanotubes · Isophorone diamine · Chlorpyrifos · Imazail · Pesticides · Water

Introduction

Crops protection against pests is one of the prevalent burdens in the agricultural sector since insects feast on plants. South Africa (SA) is one of the highest importer and user of pesticides in Africa (Bertrand 2019). Chlorpyrifos (CPF) and imazalil (IMA) are amongst the most frequently used pesticides in citrus farming worldwide (Bertrand 2019). These pesticides belong to a diverse chemical class and are amongst the top ten pesticides used for commercial citrus production (Soheilifard et al. 2020). The previous studies have indicated that excessive exposure of these pesticides on humans results in disorders such as endocrine disruption, immune impacts, genotoxicity, mutagenicity, carcinogenesis, and neurodevelopmental effects in children (Shah 2020). The use of these pesticides in citrus farming is a common exercise, and this can end up in the contamination of both the surface and groundwater. The pesticide residue reaches the dams and rivers through erosion due to an overflow (Mas et al. 2020). Other factors amounting to loss of pesticides from agricultural fields to rivers include soil property, topology, weather, chemical, and environmental properties of individual pesticides (Syafrudin et al. 2021).

Editorial responsibility: Gaurav Sharma.

✉ T. Magadzu
takalani.magadzu@ul.ac.za

[1] Department of Chemistry, University of Limpopo, Sovenga 0727, South Africa

[2] Department of Chemistry and Chemical Technology, Sefako Makgatho Health Sciences University, Ga-Rankuwa 0204, South Africa

[3] Department of Chemical Sciences, University of Johannesburg, Johannesburg, South Africa

Bodies such as Codex Alimentarius Commission (CAC), European Union (EU), and South African Department of Environmental Affairs have set the maximum residue limits (MRLs) for pesticides and their relevant transformation products in various matrices such as water, food, feed, and veterinary products (Ambrus et al. 2023). The guideline value for CPF in drinking water is set at 30 $\mu g.L^{-1}$ by CAC, whereas the MRL for IMA in water is 0.05 $mg.L^{-1}$, according to the EU commission regulation (EC) No. 396/2005. The MRLs in citrus fruits set by South African Department of Environmental Affairs for CPF and IMA are 0.05 and 5 $mg.L^{-1}$, respectively (Espana et al. 2022). This requires the developments of simple, fast, cheap, and sensitive analytical techniques for simultaneous determination of these pesticides in water and other environmental samples.

A wide range of analytical techniques such as liquid–liquid extraction (LLE), solid-phase extraction (SPE), solid-phase microextraction (SPME), stir bar sorption extraction (SBSE), liquid-phase microextraction (LPME), and quick, easy, cheap, effective, rugged, and safe (QuEChERs) has been developed in order to identify pesticides in water (Speltini et al. 2019; Dhegihan et al. 2021; Wang et al. 2021a, b). Amongst these analytical techniques, the advantages of SPE adsorbent bed are that it possesses good percentage recoveries for most pesticides (Veloo and Ibrahim 2021). Furthermore, the SPE method is highly selective towards a specific analyte of interest, which lead to enhanced recovery. Amongst various forms of adsorbent beds, the polymeric reverse phase (PRP) (a non-polar C-18 bonded to silica) is widely used to extract all forms of pesticides (Scigalski and Kosobucki 2020; Guo et al. 2021). However, these types of bed are difficult to develop and highly expensive (Maranata et al. 2021). Other SPE methods use carbon-based materials such as activated carbon (AC) to extract pesticides (Kumric et al. 2019). However, the disadvantages of AC are that it is inactive towards polar compounds and difficulty to regenerate (Kodali et al. 2021).

In order to address most of the issues noted above, the study aims to prepare a variety of multiwalled carbon nanotubes (MWCNTs)-based adsorbent beds for extraction of pesticides. MWCNTs are a unique type of carbon nano-based materials with unique physicochemical and structural properties (Alothman and Wabaidur 2019; Cho et al. 2022). Amongst other properties, MWCNTs walls can be activated by introducing various forms of active adsorption sites. These is achieved by either acid treating the MWCNTs and/or functionalising with polymeric organic compounds such as amines (Dubey et al. 2021; Salah et al. 2021). Various applications of MWCNTs as adsorbents of pesticides in water have been reported (Alothman et al. 2020; Ma et al. 2020; Rao et al. 2020). However, none of the reports investigated and compared the influence of the presence of different functional groups (such as amines and hydroxyl) on the surface of MWCNTs towards pesticides analysis.

Herein, the study aims at investigating the effects of amine-based MWCNTs adsorbent on the pre-concentration of residues of CPF and IMA in water. The prepared nanocomposite materials were characterised by powder X-ray diffraction (PXRD), scanning electron microscopy (SEM), transmission electron microscope (TEM), Brunauer–Emmet–Teller (BET), Fourier transform infrared (FTIR) spectroscopy, and thermogravimetric analysis (TGA). The isophorone diamine-modified multiwalled carbon nanotubes (IPD-MWCNTs) nanocomposite offered a simple, fast, and cheap SPE method. Its adsorption capabilities were compared with those of a pristine and oxidised MWCNTs in conjunction with a gas chromatography–mass spectrometry (GC–MS) for simultaneous determination of CPF and IMA in environmental water samples.

Materials and methods

Chemicals and materials

The MWCNTs (50–90-nm diameter, > 95% carbon basis), *N,N*-dimethylformamide, CPF and IMA analytical standards (98% purity), IPD, AC, and ethanol (absolute) were purchased from Sigma-Aldrich (St. Louis, Missouri, USA). Nylon membranes (0.45 µm), acetonitrile, methanol, chloroform, dichloromethane, *n*-hexane, and water of HPLC grade were purchased from Merck (Johannesburg, SA). Strata-X 33-µm (30 mg) PRP extraction cartridges and 0.22-µm pore sized syringe filters were purchased from Separation Scientific (Johannesburg, SA). Nitric acid (55%) and sulphuric acid (95%) were purchased from Rochelle Chemicals (Johannesburg, SA). Primary standards (100 $mg.L^{-1}$ CPF and IMA) were prepared by accurately weighing the corrected mass of each analytical standard into a 100-mL volumetric flask and filled to volume with acetonitrile. A working/secondary standards of 10 and 1 $mg.L^{-1}$ were prepared by diluting the primary standard 10 and 100 times, respectively, using a micropipette into a 10-mL volumetric flask and filled to volume with acetonitrile. Both the primary and working standards were stored in the freezer at -10 °C.

Instrumentation

Powder X-ray diffraction analysis

A PANalytical X'Pert Pro powder XRD supplied by Riga Technical University (Latvia) was used to monitor both the structures of the pristine and functionalised MWCNTs. The PXRD parameters were used as follows: Two K-alpha Cu wavelengths of 1.5405980 and 1.5444260 Å with a ratio

0.500, a divergence slit fixed at 0.38-mm monochromator, and a continuous scan range of 4.5–130, scan step size of 0.0262 with 4760 points.

Scanning electron microscopy analysis

The surface morphology analysis was studied using a JEOL 7500 SEM supplied by Thermo Fisher Scientific, Massachusetts, (USA), by capturing secondary electron images using acceleration voltage of 3 kV at the working distance of 8 mm. The images were captured in the magnification range of 1–10 µm. The sample elemental composition was measured using energy-dispersive spectroscopy (EDS).

Transmission electron microscopy analysis

A JEOL JEM 1010 TEM supplied by Thermo Fisher Scientific, Massachusetts, (USA), was used to study the morphology and microstructure of both the pristine and functionalised MWCNTs. The MWCNTs were dispersed in absolute ethanol, ultra-sonicated for approximately 2 min. Holey carbon-coated grids were dipped briefly into each CNT suspension and allowed to dry before observation.

Brunauer–Emmet–Teller analysis

A Tristar II manufactured by Micromeritics (Norcross, USA) was used for BET measurements of the pristine and functionalised MWCNTs. Prior to all measurements, samples were degassed at 300 °C for 5 h. The BET surface area, pore size, and volume were measured using nitrogen at 77 K.

Fourier transform infrared spectroscopy analysis

The FTIR spectroscopy by Spectrum 100 spectrometer supplied by Perkin Elmer (Johannesburg, SA) was used to analyse the samples in transmission mode. The FTIR spectra of the samples were obtained in the range of 500–4000 cm^{-1}. A total of 32 scans were run at a spectral resolution of 16 cm^{-1}.

Thermal gravimetric analysis

The TGA studies were carried out by a Waters TGA 5500 (New Castle, USA) in a platinum pan at a heating rate of 10 °C.min^{-1} to 900 °C under a nitrogen flow of 40 mL.min^{-1} to measure the change in mass of MWCNTs over a range of temperatures.

Gas chromatography–mass spectrometry analysis

The GC analyses were performed using a Shimadzu GCMS-QP2010 SE (Kyoto, Japan). The injection syringes were first rinsed with methanol, then rinsed with a fortified sample prior to injecting 5 µL of sample. The syringe was again rinsed with methanol post-injection to eliminate any cross-contamination. A GC capillary column InertCap with the following parameters: I.D. = 0.25 mm, length = 30 m, df = 0.25 µm, and max. temp. = 325 °C were obtained from RESTEK. A helium gas for mobile phase was obtained from AFROX. The GC oven temperature was initially held at 35 °C for 4 min and then increased to 200 °C at 15 °C/min and further increased to 300 °C at 20 °C/min and held for 5 min. The column flow was constant at 2 mL/min with an average velocity of 51.9 cm/sec and column pressure of 128.7 kPa. For mass spectrometric analysis, the interface and ion source temperatures were held at constant temperatures of 250 and 180 °C, respectively. The solvent delay was set at 2.5 min. Full scan GC–MS chromatograms were obtained by scanning from m/z of 30 to 700 amu. The ions monitored were CPF at m/z of 97 (base peak ion), 197, and 314 and IMA at m/z of 81, 173, and 215 (base peak ion). Peak areas of base peak ions were used for all quantifications.

Oxidation and functionalisation of MWCNTs

The pristine MWCNTs were primarily oxidised using a mixture of $HNO_3 + H_2SO_4$, in a ratio of 1:3 (v/v) following an existing method (Mkhondo and Magadzu 2014). The resultant oxidised MWCNTs were treated with IPD as follows: Briefly, approximately 0.200 g of oxidised MWCNTs was mixed with 1.00 g of IPD in 200 mL *N,N*-dimethylformamide and refluxed at 180 °C for 92 h. The resultant amine functionalised MWCNTs composite was washed numerous times with 95% ethanol to remove any surplus uncrafted amines. The solid product was collected using a 0.45-µm pore sized membrane and dried in an oven for 6 h at 60 °C.

MWCNTs cartridge assembling and adsorption studies

The MWCNTs-packed SPE cartridges were assembled by placing 30-mg MWCNTs nanocomposite in an empty polypropylene SPE cartridge (3-mL Strata-X 33 cartridge from Separations). This was held in place in the polypropylene SPE cartridge using upper and lower polypropylene sheet with 20-µm pore. The cartridge was firstly conditioned with 10-mL acetone followed by 10-mL deionised water. A 100 mL of fortified/pesticide-free water sample was passed through the cartridge at a constant flow rate of 1 mL.min^{-1} in a vacuum manifold. The loaded cartridges were vacuumed to dryness and thereafter washed with 10 mL of petroleum ether to remove any co-adsorbed matrix materials with the aim of not interfering with the target analytes. Thereafter, the retained analytes were eluted into a 15-mL test tube. The resultant eluent was gently evaporated to near dryness under N_2 *(g)* at 60 °C. The dry residue was reconstituted with 2-mL

acetonitrile, vortexed for a minute, filtered through a 0.22-µm pore sized syringe filter, and transferred to a 2-mL sample vial. About 5 µL of the extracts were injected onto a GC–MS for analysis.

Water sample collection procedure

Water samples were obtained from Bon Accord Dam (Pretoria, South Africa) for pesticide residue analysis. The water samples were collected in brown bottles and stored at 4 °C in a refrigerator for further analysis. Approximately, 100 mL of water samples were filtered through a 0.45-µm membrane filter before use.

Method validation

Validation of the analytical method was conducted by evaluating analytical figures of merit that includes linearity, precision, accuracy, limit of detection (LOD), and limit of quantification (LOQ).

Linearity

The linearity was evaluated by constructing calibration curves for CPF and IMA in the concentration range: 0.05–1.000 mg.L^{-1} in water. The spiking levels were guided by the permissible maximum residue limit (MRL) of these pesticides in water which is 1.000 mg.L^{-1}. This method was able to include values far below $^{1}/_{2}$MRL. Analysis of each point was performed in triplicate, and average values were used. The calibration curves were generated by plotting peak area of CPF and IMA against their concentrations. The linearity of the method was determined from the calibration curve by calculating the correlation coefficient, slope, and intercept values.

Precision

The method precision was assessed in terms of intra-day and inter-day precision, where the percentage relative standard deviation (%RSD) of less than 20% was used as criteria. This was verified from repetitions of low, medium, and high concentrations of CPF and IMA (0.050, 0.400, and 1.000 mg.L^{-1}). Inter-day measurements for the reproducibility were performed on 4 consecutive days.

Accuracy

The closeness between the expected and calculated values of the method was calculated in terms of percentage recovery (%R) using Eq. (1).

$$\%R = \frac{C_2}{C_1} x100 \tag{1}$$

where C_1 is the known CPF and IMA concentrations, and C_2 is the calculated CPF and IMA concentrations in the water sample. The water samples were spiked at three different concentration levels of low, medium, and high (0.05, 0.40, and 1.0 mg.L^{-1}). Recovery experiments were performed with five repetitions.

Limits of detection and quantification

The LOD and LOQ were determined using the calibration curve by first determining the peak area experimentally (Y) and by calculation (X). Thereafter, the standard deviation (SD) was calculated using these values in Eq. (2).

$$SD = \sqrt{\frac{\Sigma(Y - X)^2}{n - 2}} \tag{2}$$

Thereafter, the LOD and LOQ values were achieved using Eqs. (3) and (4), respectively.

$$LOD = \frac{3xSD}{m} \tag{3}$$

$$LOQ = \frac{10xSD}{m} \tag{4}$$

where n is the number of standards used, and m is the slope of the calibration curve.

Results and discussion

The results and discussion are arranged in the following manner: The first segment presents the characterisation of the pristine, oxidised, and IPD-MWCNTs. The aim of this segment was to examine and discuss the effects of the modification processes and the accomplishment thereof. The second segment investigates the performance of the characterised nanocomposites when applied as adsorbents of CPF and IMA in water as well as optimisation of the superior nanocomposite.

Characterisations

Powder X-ray diffraction analysis

The PXRD patterns of the pristine, oxidised, and IPD-MWCNTs were obtained to examine if any form of structural destruction occurred during the purification and/or functionalisation. The PXRD profiles in Fig. 1 show the diffraction patterns of (a) pristine, (b) oxidised, and (c) IPD-MWCNTs.

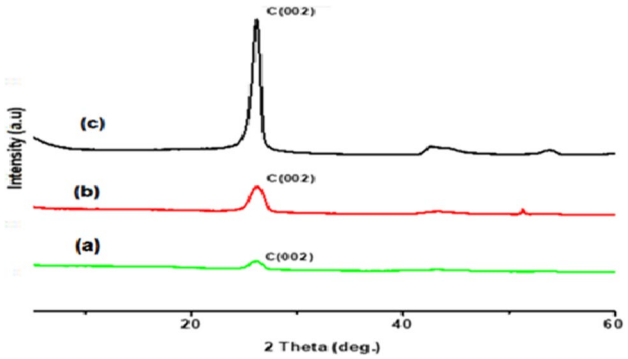

Fig. 1 PXRD patterns of **a** pristine, **b** oxidised, and **c** IPD-MWCNTs

The three diffraction patterns show the same characteristic peak at 2θ = 26°, which corresponds to (002) reflection planes. The intensity of the characteristic peak (002) is lower on pristine MWCNTs (Fig. 1a). This is attributed to poor dispersity and bundling of the pristine MWCNTs (Sabri et al. 2019). Upon acid treatment, the intensities of oxidised MWCNTs (Fig. 1b) increased slightly. This indicates that there is an unbundling of MWCNTs and removal of impurities as observed on TEM and EDS data. Interestingly, the XRD pattern of IPD-MWCNTs (Fig. 1c) gave a highly intense sharp peak, which clearly suggests an intact and ordered structure of MWCNTs (Alothman et al. 2020).

The patterns of the treated MWCNTs show the presence of some unsymmetrical carbons (at 2θ = 51°) normally referred to as diaphanous carbons that form during various stages of material purifications (Chowdhry et al. 2019).

Scanning electron microscopy and transmission electron microscopy

SEM was undertaken to assess the surface morphology of the prepared MWCNTs composite materials. The data in Fig. 2 show the SEM images of (a) pristine, (b) oxidised, and (c) amine functionalised MWCNTs. The SEM images of the three MWCNTs show a similar uppermost layer made up of an unsystematically oriented network of tubes (Piao et al. 2021). The surface structure of the MWCNTs was further investigated using TEM, and images of (a1) pristine, (b1) oxidised, and (c1) IPD-MWCNTs are shown in Fig. 2. All TEM images do show that the structure of MWCNTs remained intact upon oxidation (Fig. 2b1) and functionalisation by an isophorone diamine (Fig. 2c1). The oxidised MWCNTs (Fig. 2b1) show some spherical-shaped inner tubes, which indicates that diaphanous carbons were removed as compared to that of pristine MWCNTs (Fig. 2a1), hence unclogged the walls of MWCNTs. Some few remaining residual carbon-encapsulated catalytic metal particles are also observed in Fig. 2b1, represented by black circular spots (Patel et al. 2020; Bajorek et al. 2022).

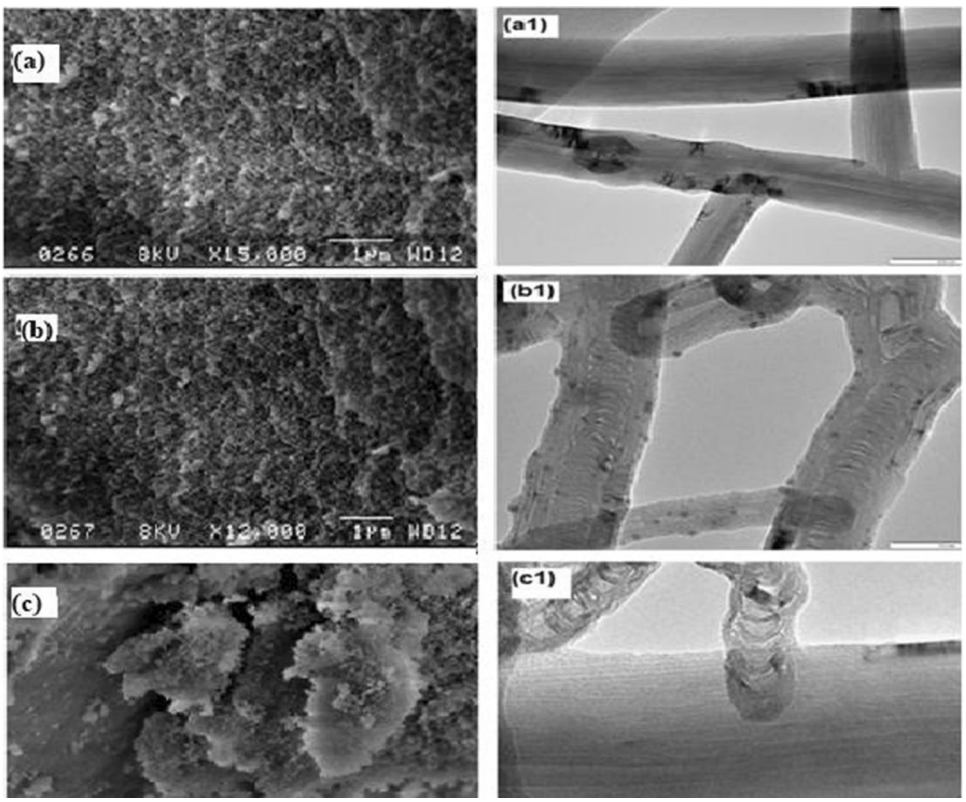

Fig. 2 SEM images of **a** pristine, **b** oxidised, and **c** IPD-MWCNTs and their corresponding TEM images (a1, b1, and c1)

Energy-dispersive X-ray spectroscopy

The data in Fig. 3 show the EDS spectra of (a) pristine, (b) oxidised, and (c) IPD-MWCNTs. The weight % of the carbon content for the pristine MWCNTs was found to be 95.27%. However, upon oxidation, the oxidised MWCNTs (Fig. 3b) showed a decrease of about 10.53% of carbon content as compared to pristine MWCNTs (Fig. 3a). This is because of the selective removal of some metallic particles and the creation of some diaphanous carbons (Alotaibi et al. 2021; Grinberg et al. 2022). This finding further supports the observed TEM images of oxidised MWCNTs. Upon functionalisation with IPD, an increase in the carbon content of the IPD-MWCNTs (98.74%), reduction of the oxygen content (0.06%), and an increase in nitrogen content (1.10%) were observed (Fig. 3c). The decrease in oxygen content is linked to the replacement of oxygen by amine groups during functionalisation. Furthermore, the EDS spectra of the oxidised and IPD-MWCNTs show the disappearance of some metallic impurities. These metallic impurities are normally formed during MWCNTs production (Nawarathne et al. 2021; Sun et al. 2021; Tserengombo et al. 2021).

Brunauer–Emmet–Teller analysis

The BET-specific surface areas (SSA), pore volume, and average particle size of the pristine, oxidised, and IPD-MWCNTs are presented in Table 1. The BET-SSA of the pristine MWCNTs is 22.3 $m^2.g^{-1}$ and upon acid treatment, the SSA of the oxidised MWCNTs increased to 25.1 $m^2.g^{-1}$. An increase in BET-SSA can be attributed to the removal of some metallic particles, amorphous carbons, and introduction of defects sites on the walls of oxidised MWCNTs (Rodriguez and Leiva 2020). These findings are supported

Table 1 Surface characteristics of pristine, oxidised, and IPD-MWCNTs

Sorbent type	BET-specific surface area ($m^2.g^{-1}$)	Pore volume ($cm^3.g^{-1}$)	Average particle size (Å)
Pristine MWCNTs	22.3	0.036578	2687.78
Oxidised MWCNTs	25.1	0.033554	2386.02
IPD-MWCNTs	25.7	0.040555	2335.91

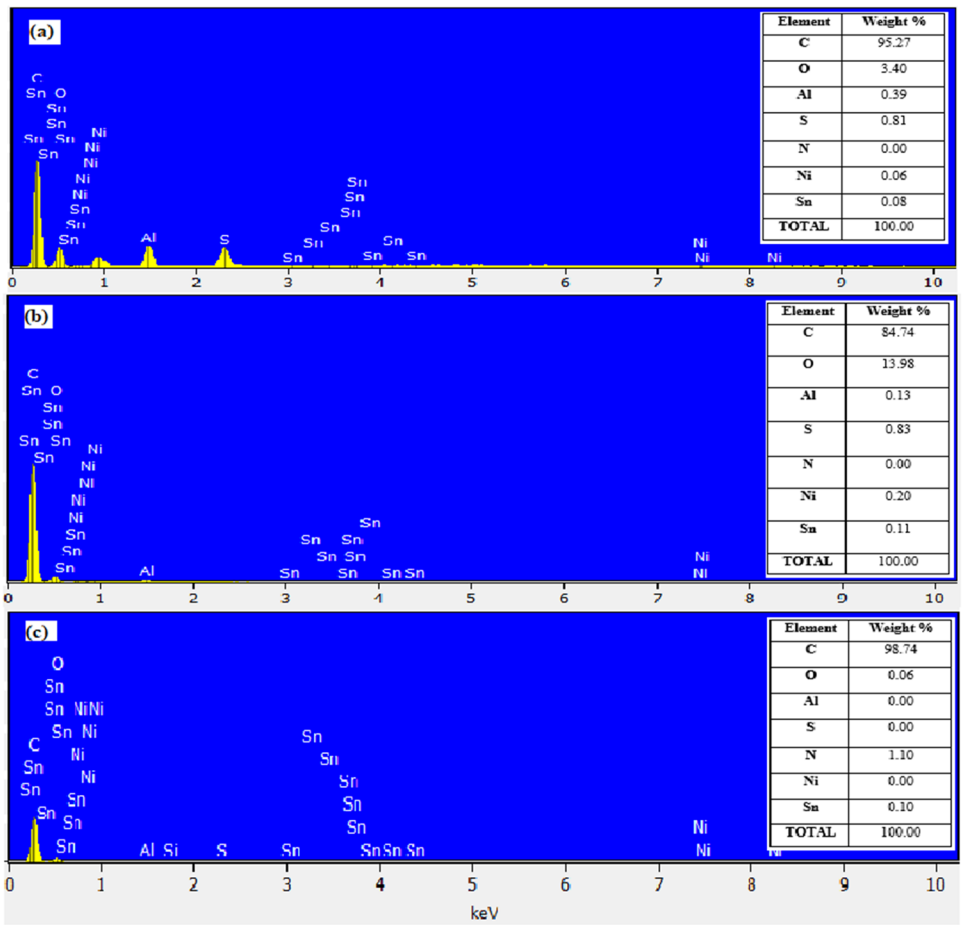

Fig. 3 EDS of **a** pristine, **b** oxidised, and **c** IPD-MWCNTs

by the EDS spectra, which indicated the disappearance of most metallic particles post acid treatment. Sonication of the composites with a solvent such as the *N,N*-dimethylformamide (DMF) also contributed to the dispersity and hence an improvement of BET-SSA of oxidised MWCNTs (Wang and Pang 2020).

A further functionalisation of the oxidised MWCNTs with IPD showed an increase in the BET-SSA which was measured to be 25.7 $m^2.g^{-1}$. This further demonstrates a successful crafting of the IPD onto the walls of the MWCNTs. The addition of IPD on the surface of MWCNTs is expected to further increase the active sites within the structure of the composite (Plunkett et al. 2019; Basivi et al. 2021). There is a slight difference in pore volume between the pristine and oxidised MWCNTs; however, a noticeable increase has occurred on IPD-MWCNTs composite.

Fourier transform infrared spectroscopy analysis

The data in Fig. 4 show an FTIR spectra of (a) pristine, (b) oxidised, and (c) IPD-MWCNTs. Treatment of MWCNTs with oxoacids generates some form of oxygenated functional groups (– COOH, C = O, and C-O–O) located on the walls. A successful generation of these functional groups allows further modifications on the oxidised MWCNTs by introducing other functional groups such as amines (Kashyap et al. 2020). In this case, FTIR spectroscopy was used to characterise the functional groups present on the surfaces of the pristine, oxidised, and IPD-MWCNTs. The characteristic bands for CNTs are located between 1900 and 2100 cm^{-1} of Fig. 4 (Sreejarani et al. 2011). This band remained visible in the three MWCNTs demonstrating the conservation of the graphite structure of the MWCNTs.

The FTIR spectra of oxidised (Fig. 4b) and IPD-MWCNTs (Fig. 4c) contain a broad band at around 3400 cm^{-1} representing the stretching vibrations of isolated surface –OH moieties in carboxyl groups and/or –NH in amine groups. The band at 2900 cm^{-1} on pristine MWCNTs (Fig. 4a) confirms the presence of asymmetric/symmetric C–H normally located at the defected sides of the MWCNTs (Kodali et al. 2021). The C-O bands from the carboxyl groups (C–O and COO^-) are observed in the range 1500–1700 cm^{-1} of Fig. 4b and c (Salah et al. 2021; Sibaja et al. 2021). The IPD-MWCNTs contain peaks between 1100 and 1200 cm^{-1}, which correspond to the presence of C–N and N–CH_3 (Tripani et al. 2020; Thi and Hoa 2021; Bajorek et al. 2022). The presence of this amino group stretch on the FTIR spectra confirms a successful functionalisation of IPD on the walls of MWCNTs.

Thermal gravimetric analysis

The data in Fig. 5 show TGA profiles of (a) pristine, (b) oxidised, and (c) IPD-MWCNTs. The TGA profile of pristine MWCNTs (Fig. 5a) shows a single-stage decomposition that occurred at 800 °C, which is typical for MWCNTs (Risoluti et al. 2020). The weight loss observed on the oxidised MWCNTs (Fig. 5b) at 600 °C is attributed to the loss of oxygen-containing functional groups. Furthermore, the defects that are mainly produced during oxidation could have contributed to instability of the oxidised MWCNTs (Sezer and Koc 2019; Kim et al. 2022; Saidi et al. 2022). The TGA profile of IPD-MWCNTs (Fig. 5c) shows a weight loss at 300 °C which is attributed to the decomposition of the IPD organic compound attached to the walls of MWCNTs (Silva et al. 2012; Massoumi et al. 2019). The profile depicts that the addition of easily combustible heteroatoms such as hydroxyl groups or IPD compounds compromises the thermal stability of the entire MWCNTs nanocomposite.

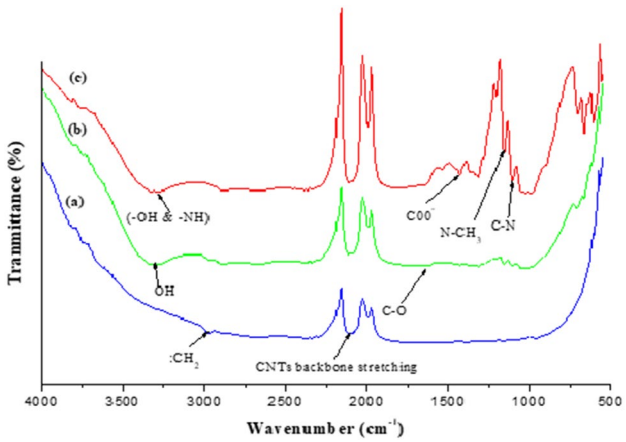

Fig. 4 FTIR spectra of **a** pristine, **b** oxidised, and **c** IPD-MWCNTs

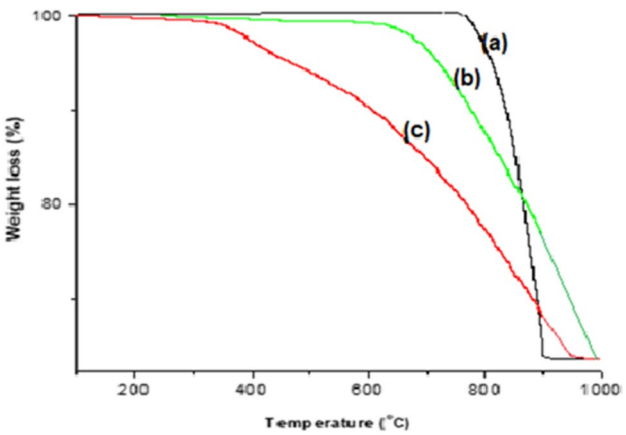

Fig. 5 TGA profiles of **a** pristine, **b** oxidised, and **c** IPD-MWCNTs

Application of the pristine, oxidised, and IPD-MWCNTs as SPE adsorbents

Factors that influence the realisation of an effective SPE procedure and overall analyte adsorption were optimised. These factors included adsorbent type and mass, eluent type and its volume, and the reusability of the adsorbent. Therefore, a careful stepwise procedure had to be followed for a successful SPE of CPF and IMA pesticides in water. These optimisation studies were performed on the adsorbent that is envisaged to possess outstanding analyte recoveries in water samples. The ultimate method was tested in environmental water samples, and all measurements were performed in triplicates.

The effects of the adsorbent type towards the recovery of CPF and IMA

The determination of good adsorbents for specific target analytes is crucial since different sites on CNTs (based on compounds used for functionalisation) have different affinities. A pristine, oxidised, and IPD functionalised MWCNTs were applied as adsorbents to determine which of these nanocomposites provide the best analyte recovery. The data in Fig. 6 show the extraction capabilities of the (a) pristine, (b) oxidised, and (c) IPD-MWCNTs. The results show that the retention of CPF remained higher as compared to that of IMA on all adsorbent, throughout the recovery experiments. However, the IPD-MWCNTs showed better recoveries for both analytes, followed by the oxidised MWCNTs, and then the pristine MWCNTs. This indicates that IPD-MWCNTs have a better analyte retention efficiency; a related finding was observed by Wang et al. 2021a, b, using tetraethylenepentamine-modified MWCNTs towards the extraction of pesticides. The observed analyte recovery by IPD-MWCNTs is attributed to increased number of active sites for adsorption and a higher BET-specific surface area (Hoa 2021; Abdullah et al. 2021).

Determination of elution solvent

The determination of the composition of an elution solvent (eluent) is one of the imperative steps when developing any good SPE procedure. This is because the target analytes ought to be effectively eluted with the least possible interferences. The polarities of analytes and elution solvent play an important role during elution (Gulati et al. 2020; Nawaz et al. 2020). In this study, six different organic solvents with different polarities that include acetonitrile (ACN), chloroform ($CHCl_3$), dichloromethane (DCM), methanol (MeOH), ethanol (EtOH), and *n*-hexane were separately investigated as eluents to determine their individual strength to elude the selected analytes. The data in Fig. 7 show the elution of CPF and IMA on an IPD-MWCNTs adsorbent during SPE using the outlined eluents. The data indicate the following trend of analyte elution of CPF: EtOH > $CHCl_3$ > *n*-hexane > MeOH > ACN > DCM and IMA: $CHCl_3$ > EtOH > MeOH > ACN > and *n*-hexane > DCM, respectively. The trend indicates that the two analytes are best eluted using EtOH and $CHCl_3$, which comprises diverse polarity indexes. Therefore, it was essential to evaluate the effects of their combination towards the elution of the two analytes.

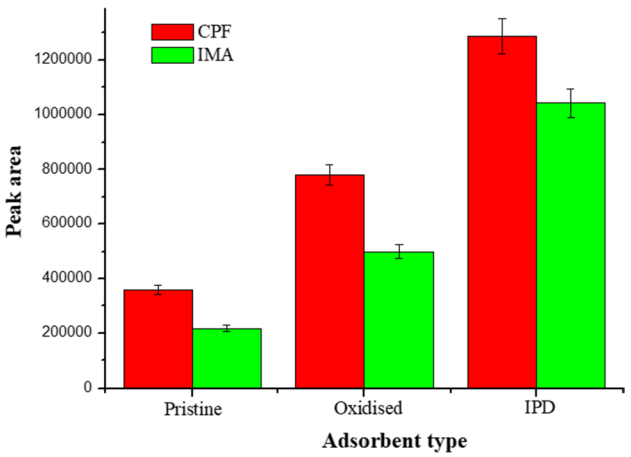

Fig. 6 Effects of **a** pristine, **b** oxidised, and **c** IPD-MWCNTs sorbents on the recoveries of 1.0 $mg.L^{-1}$ CPF and IMA spiked in 100-mL water sample (Conditions: adsorbent mass = 30 mg and eluent = 4-mL acetonitrile)

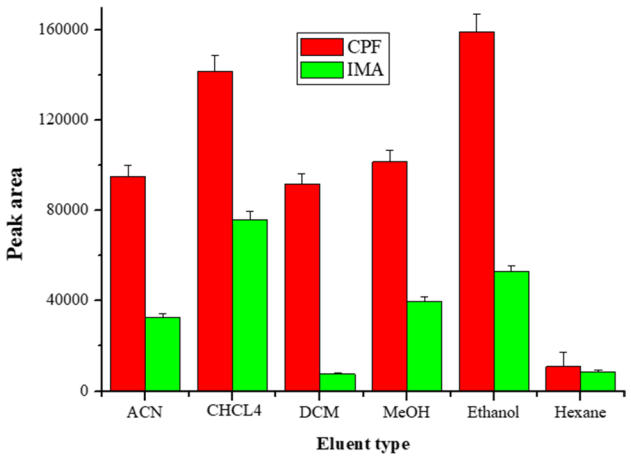

Fig. 7 Effects of different eluents on the recovery of 1.0 $mg.L^{-1}$ CPF and IMA in 100-mL water sample (Conditions: eluent = 4-mL solvent and adsorbent mass = 30-mg IPD-MWCNTs)

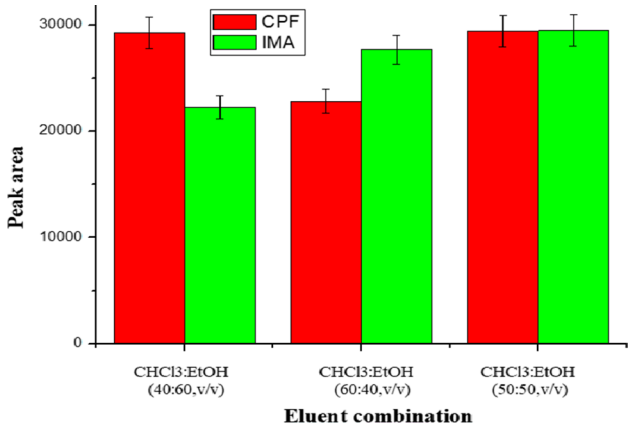

Fig. 8 Effects of $CHCl_3$:EtOH (40:60; 60:40; and 50:50, v/v) solvent combination on the recoveries of 1.0 $mg.L^{-1}$ CPF and IMA in 100-mL water sample (Conditions: eluent volume = 4 mL and adsorbent mass = 30-mg IPD-MWCNTs)

The effects of combining EtOH and $CHCl_3$ solvents towards the recovery CPF and IMA

The data in Fig. 8 show the effects of combined solvents (EtOH and $CHCl_3$) towards the recovery CPF and IMA from water samples. Although the two solvents are homogenously combined, it does not necessarily suggest that they are homogeneous but rather cumulate and form a microscopic solvent combination. The results show that when the solvent combination ratio is $CHCl_3$:EtOH (40:60, v/v), the recovery of CPF is greater than that of IMA. However, when the ratio is interchanged, the recovery of IMA is greater than that of CPF. This outcome motivated the use of equal combination of both elution solvents at a ratio of 50:50 (v/v). When the ratios are equal, the combined elution solvent yielded relatively similar recoveries for both pesticides. The elution capabilities of chloroform were not unexpected since both pesticides are highly chlorinated compounds. Subsequently, the ultimate performance of ethanol may also be attributed to its polarity in comparison with both pesticides. Therefore, the combined elution solvent ($CHCl_3$:EtOH, 50:50 v/v) was preferred due to their different polarity indexes (Jajuli et al. 2021).

Determination of elution volume

The volume of the solution used to elute analytes from a SPE adsorbent bed (an elution volume) has a direct and measurable effect on the overall procedure. This is because it is a key variable necessary to completely remove all the analytes from the adsorbent bed. Therefore, a sufficient amount of elution solvent must be determined in order to obtain maximum recovery of the retained analytes from the adsorbent bed. This effect was investigated by using different volumes of a previously determined eluent (50:50, v/v $CHCl_3$:EtOH). In this case, the eluent volumes were varied between 2 and 8 mL, and the results are shown in Fig. 9. The recoveries of both analytes increased with an increase in the volume of eluent from 2 to 6 mL. The results indicate that as the eluent volume increases, it distributes through the adsorbent bed, and the analytes are alternatively adsorbed and desorbed to lower positions as the movement of the eluent continues (Maranata et al. 2021). All analytes were recovered within the 6-mL volume, and as a result, this was preferred as the elution volume for subsequent experiments.

The effects of adsorbent dosage

It is expected that, as the adsorbent dosage increases while keeping other parameters constant, the adsorbent efficacy will also increase until it reaches maximum. In this procedure, different sorbent masses of IPD-MWCNTs ranging from 0.015 to 0.150 g were investigated. The data in Fig. 10 show that as the adsorbent dosage increases from 0.015 to 0.030 g, the adsorbent efficiency also increased towards the recovery of both analytes. The adsorbent bed with the lowest mass (0.015 g) recovered lesser amounts of both analytes. The lower recoveries indicate that few target analytes were adsorbed on the adsorbent bed; of which its active adsorption sites get saturated quickly. However, as the adsorbent dosage increased to 0.030 g, the recovery of both analytes increased. This is linked with an increase in adsorption sites, hence the improved recovery (Selambakkannu et al. 2019). The recovery remained relatively the same with a slight decrease in analyte recovery as the adsorbent mass was increased above 0.030 g. This dosage is very small as compared to the reported 0.500-g conventional SPE cartridge as well as 0.100-g MWCNTs previously used to recover pesticides in water (Huq 2011; Atrache et al. 2016).

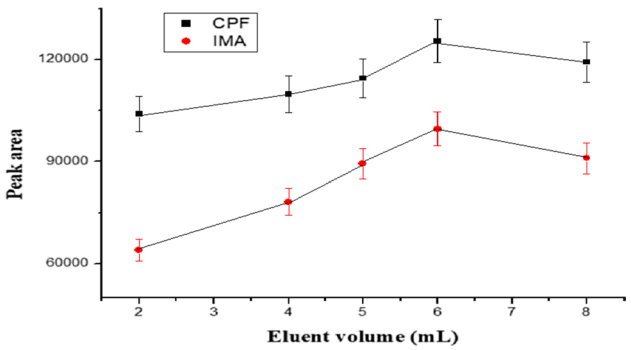

Fig. 9 Effects of eluent volume on the recovery of 1.0 $mg.L^{-1}$ CPF and IMA in 100-mL water sample (Conditions: adsorbent mass = 30-mg IPD-MWCNTs; eluent = 50:50 v/v $CHCl_3$:EtOH; and eluent volume = 2.00–8.00 mL)

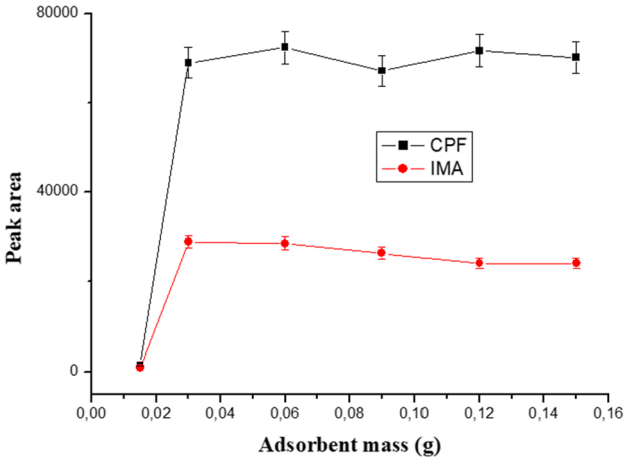

Fig. 10 Effects of sorbent mass on the recovery of 1.0 mg.L^{-1} CPF and IMA in 100-mL water sample (Conditions: eluent = 6 mL of 50:50 v/v $CHCl_3$:EtOH and adsorbent mass = 0.015–0.150-g IPD-MWCNTs)

Reusability of IPD-MWCNTs

The feasibility to reuse IPD-MWCNTs without substantial impact on the retention capacity of the adsorbent bed has been tested. This was done by using a single adsorbent dosage to extract target analytes from more than one fortified water samples as shown in Fig. 11. The results show relatively the same recoveries, when a single IPD-MWCNTs adsorbent was reused several times. This was achieved following appropriate reconditioning of the entire SPE cartridge. The seven repeated cycles of a single IPD-MWCNTs adsorbent produced an acceptable %RSD ranging from 3 to 8%, for recovery of both analytes. These %RSD ($\leq$20%) values are acceptable according to the set limits and therefore support the precision for the reusability of the IPD-MWCNTs as an adsorbent (SANTE 2015). These data indicate that the IPD-MWCNTs are highly stable, and its active sites cannot be easily fouled, as compared to the acid-treated MWCNTs adsorbent reported by Barbosa et al. 2020 and Gholami et al. 2022.

Analytical figures of merit

Method validation

Calibration curves for both CPF and IMA in spiked pesticide-free water samples were constructed to evaluate the linearity, recovery, repeatability, and limits of detection and quantification for the developed method. The fortified calibration curves for the pesticide-free samples are shown in Fig. 12. The calibration curves obtained were all linear with regression equations $y = 30624x + 20{,}702$ (CPF) and $y = 3121x$–20,443 (IMA) and their coefficient of determination (R^2) values of 0.99151 and 0.99866, respectively. These linearities were obtained in the concentration range of 0.050–1.000 mg.L^{-1} for both analytes with at least three replicates for each point. The average % recoveries obtained were 97% for CPF and 112% for IMA. These % recoveries fall within trueness range of 70–120% for each fortification level according to the SANTE 2015 guidelines. This confirms the trueness of the method within their respective spiking levels and also suggests its suitability to be used at levels far below that of half-MRL of the two analytes in water.

Precision

The intra-day and inter-day precision of the method was determined by SPE of spiked water samples using the IPD-MWCNTs at low, medium, and high concentrations of CPF and IMA. The results obtained are outlined in Tables 2 and 3, respectively. The %RSD values of intra-day precision for CPF and IMA at concentration levels 0.05, 0.40, and

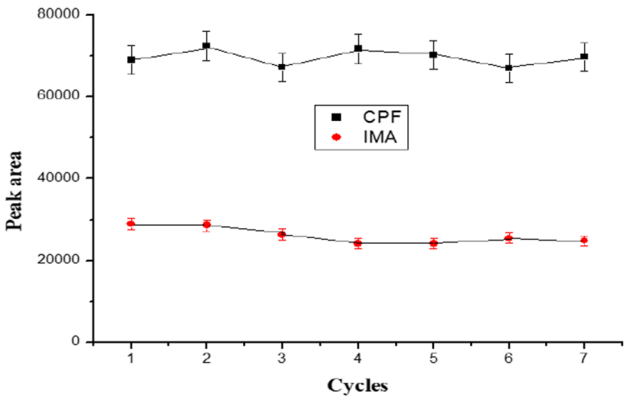

Fig. 11 Adsorbent reusability on the recovery of 1.0 mg.L^{-1} CPF and IMA in 100-mL water sample (Conditions: eluent = 6 mL of 50:50 v/v $CHCl_3$:EtOH and adsorbent mass = 0.030-g IPD-MWCNTs)

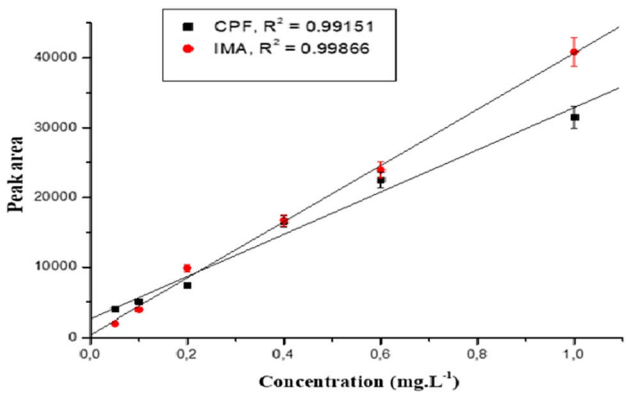

Fig. 12 CPF and IMA spiked calibration curves in 100-mL water samples (Conditions: eluent = 6 mL of 50:50 v/v $CHCl_3$:EtOH and adsorbent mass = 0.030-g IPD-MWCNTs)

1.00 mg.L^{-1} were found to be 8, 6, and 7% for CPF and 10, 6, and 3% for IMA, respectively (Table 2). The %RSD values of inter-day precision for CPF and IMA at concentration levels 0.05, 0.40, and 1.00 mg.L^{-1} were found to be 4, 3, and 1% for CPF and 3, 1, and 2% for IMA, respectively (Table 3). The obtained %RSD values of less than 20% indicate a good precision of the developed method.

Accuracy

Accuracy of the method was reported as percentage recovery by spiking low, medium, and high concentrations (0.05, 0.40, and 1.00 mg.L^{-1}) of CPF and IMA in 100-mL water samples, and the process was repeated five times. All percentage recoveries were calculated as described under methodology, and this is summarised in Table 4. The percentage recoveries determined from low, medium, and high concentration fall within the fortified calibration curve. This confirms that the trueness of the method falls within their respective spiking levels. This also suggests that this method is suitable to be used at levels way below that of half-MRL of both CPF and IMA pesticides in water samples.

Limits of detection and quantification

The LOD and LOQ for both CPF and IMA were calculated as described under the methodology. The LODs of CPF and IMA are 0.026 and 0.033 µg.L^{-1}, respectively, and their corresponding LOQs are 0.078 and 0.100 µg.L^{-1}. These lower values show that the method is able to detect and quantify

Table 2 Intra-day precision

Low conc. 0.05 mg.L^{-1}			Medium conc. 0.40 mg.L^{-1}			High conc. 1.00 mg.L^{-1}		
Repetitions	CPF	IMA	Repetitions	CPF	IMA	Repetitions	CPF	IMA
a	0.046	0.043	a	0.481	0.473	a	1.271	0.962
b	0.046	0.051	b	0.418	0.477	b	1.090	1.033
c	0.049	0.041	c	0.445	0.447	c	1.129	1.000
d	0.054	0.047	d	0.453	0.416	d	1.124	0.967
Average	0.049	0.046	Average	0.449	0.453	Average	1.153	0.991
SD	0.004	0.004	SD	0.026	0.028	SD	0.080	0.033
%RSD	8	10	%RSD	6	6	%RSD	7	3

Table 3 Inter-day precision

Low conc. 0.05 mg.L^{-1}			Medium conc. 0.40 mg.L^{-1}			High conc. 1.00 mg.L^{-1}		
Repetitions	CPF	IMA	Repetitions	CPF	IMA	Repetitions	CPF	IMA
a	0.049	0.046	a	0.486	0.483	a	1.097	1.000
b	0.050	0.049	b	0.510	0.477	b	1.097	1.000
c	0.051	0.049	c	0.479	0.478	c	1.112	0.994
d	0.046	0.049	d	0.480	0.483	d	1.099	1.042
Average	0.049	0.048	Average	0.489	0.480	Average	1.101	1.009
SD	0.002	0.001	SD	0.014	0.003	SD	0.007	0.022
%RSD	4	3	%RSD	3	1	%RSD	1	2

Table 4 Evaluation of accuracy of the method

Low conc. 0.05 mg/L			% Recovery		Medium conc. 0.40 mg/L		% Recovery		High conc. 1.00 mg/L		% Recovery	
Reps	CPF	IMA	CPF	IMA	CPF	IMA	CPF	IMA	CPF	IMA	CPF	IMA
A	0.048	0.047	96	95	0.411	0.474	103	119	1.097	1.000	110	100
B	0.047	0.048	93	97	0.425	0.477	106	119	1.097	1.000	110	100
C	0.049	0.050	99	101	0.479	0.478	120	119	1.112	0.994	111	99
D	0.045	0.052	90	105	0.480	0.471	120	118	1.099	1.042	110	104
E	0.048	0.047	96	94	0.426	0.462	107	116	1.096	0.993	110	99
Av	0.047	0.050	94	99	0.449	0.475	112	119	1.101	1.009	110	101
SD	0.002	0.002	0.038	0.044	0.036	0.003	0.090	0.008	0.007	0.022	0.007	0.022
%RSD	4	4	4	4	8	1	8	1	1	2	1	2

Table 5 LOD and LOQ values for CPF and IMA

Analyte	Current method		Literature		References
	LOD (μg.L^{-1})	LOQ (μg.L^{-1})	LOD (μg.L^{-1})	LOQ (μg.L^{-1})	
CPF	0.026	0078	0.494	1.648	(Schwantes et al. 2020)
IMA	0.033	0.100	10.00; 25.00	25.00	(Su and Lin 2003; Freitas et al. 2023)

Table 6 Spiking levels of different adsorbents (IPD-MWCNTs, PRP, and AC) and their resultant recoveries

Sorbent type	Spiking level (mg.L^{-1})	Peak area CPF	Peak area IMA	Conc Found CPF	Conc Found IMA	% Recovery CPF	% Recovery IMA
IPD-MWCNTs	0.050	3849	2011	0.050	0.040	92	80
PRP	1.000	35,468	40,838	1.070	1.000	107	100
AC	0.050	1277	–	16.75	–	34	–
	1.000	30,082	30,943	0.900	0.760	90	76
	0.050	–	–	–	–	–	–
	1.000	–	–	–	–	–	–

pesticides at low concentration when compared to several reported methods in water samples as shown in Table 5 (Su and Lin 2003; Tankiewicz et al. 2019; Schwantes et al. 2020). The obtained LOD and LOQ values show a major enhancement in the development of the current method. These values are also below the MRLs for the two analytes in water. Therefore, this method can be applied for monitoring and control of the residues of CPF and IMA in water.

Comparison of the adsorption efficiencies of IPD-MWCNTs, PRP, and AC

Adsorption capabilities of the IPD-MWCNTs were evaluated against polymeric reverse phase (PRP) and activated carbon (AC) as shown in Table 6. AC has showed extremely low and incomparable percentage recoveries for both analytes at 0.05 and 1.0 mg/L spiking levels. The low adsorption capabilities of AC may be due to their low specific surface area of 13.8 $m^2.g^{-1}$, as compared to 25.7 $m^2.g^{-1}$ of IPD-MWCNTs. Some extraction methods using AC obtained realistic percentage recoveries when analysing pesticides in tomatoes and water, respectively (Kodali et al. 2021). The additional adsorbent mass in their studies supplemented the lower specific surface area of the AC. The adsorbent capabilities of IPD-MWCNTs and PRP are shown in Fig. 13.

The data in Fig. 13 show that IPD-MWCNTs obtained higher percentage recoveries for both analytes (CPF: 92% and 107%; IMA: 80% and 100%) at low and high concentrations. The PRP showed comparable results at high concentration levels (CPF: 90% and IMA: 76%) and poor recoveries at lower levels (CPF: 34% and IMA: 0%). The PRP is an ideal competitor for most SPEs owing to its ability to be used as an all-purpose, strongly hydrophobic, reversed-phase polymer used for either acidic, basic, and/or neutral analytes

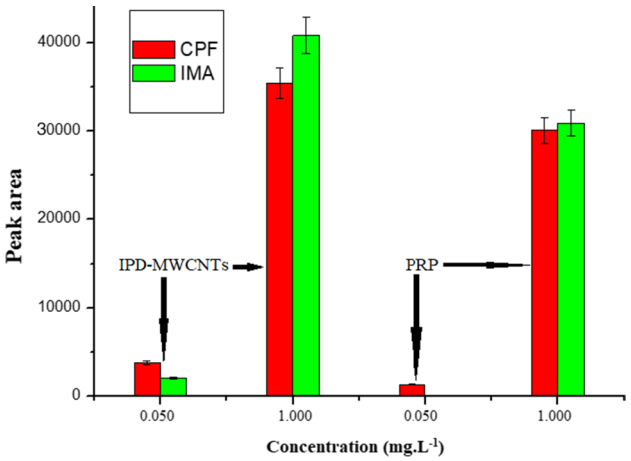

Fig. 13 Evaluation of efficacy of IPD-MWCNTs, PRP, and AC adsorbents (Conditions: eluent = 6 mL of 50:50 v/v $CHCl_3$:EtOH and adsorbent mass = 0.030-g IPD-MWCNTs)

(Badawy et al. 2022). However, the current IPD-MWCNTs-based SPE method has shown quantitative recoveries at both concentration levels and can be applied for pre-concentration of ultra-trace levels of CPF and IMA in water prior to quantification by GC–MS.

Application

The performance of the IPD-MWCNTs adsorbent was scrutinised by adsorption of CPF and IMA in real water samples. The data in Fig. 14 show the chromatograms of (a) spiked dam water, (b) non-spiked dam water, and (c) pesticide-free water sample. The overlaid chromatograms of an IPD-MWCNTs adsorbent show its ability to recover the spiked pesticides from real dam water samples. The absence

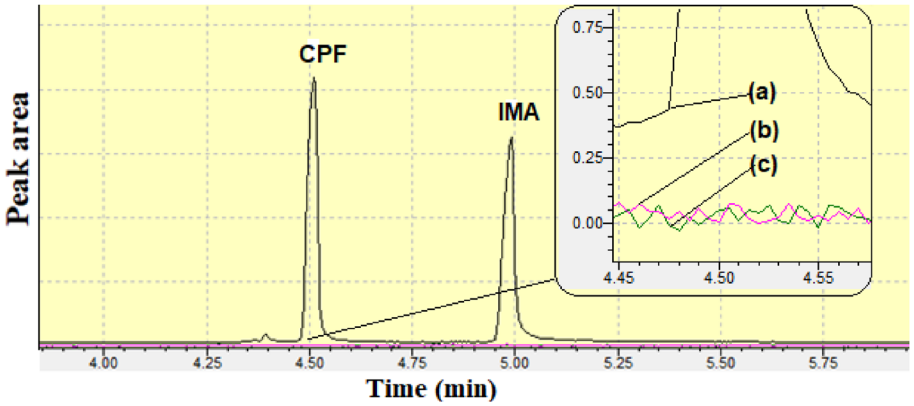

Fig. 14 Overlaid chromatograms of (a) spiked dam water, (b) non-spiked dam water, and (c) pesticide-free water samples (Conditions: eluent = 6 mL of 50:50 v/v $CHCl_3$:EtOH and adsorbent mass = 0.030-g IPD-MWCNTs)

of CPF and IMA peaks (Fig. 14b and c) is an indication that none of the two pesticides was present in the non-spiked dam and pesticide-free water samples. Overall, the ability to recover the spiked pesticides from the dam water by the IPD-MWCNTs affirms its efficiency and applicability to be used as a SPE adsorbent of pesticides in environmental water samples (Wang et al. 2021a, ba, b; 2021a, ba, b; 2022).

Conclusion

The XRD and FTIR confirm that both oxidised and IPD-MWCNTs were successfully prepared, and their structures showed improved and highly intense sharp peaks, characteristic of intact and ordered structure. Furthermore, their TEM images showed clear spherical-shaped inner tubes, which indicate that diaphanous carbons and clogged walls of MWCNT were removed; this is further supported by EDS data. The BET showed a high surface area of oxidised MWCNTs, which further improve upon functionalisation with amine compound (IPD-MWCNTs). The TGA profile of IPD-MWCNTs confirmed the presence of amine, and the nanocomposite was found to be highly stable within the pesticides quantification operating temperature.

The CPF and IMA analytes are best recovered using a low dosage of IPD-MWCNTs adsorbent (0.030 g), while using a 6 ml of combined elution solvent (i.e. EtOH and $CHCl_3$ (50:50, v/v)). The IPD-MWCNTs adsorbent was found to be reusable over seven repeated cycles, with an acceptable %RSD ranging from 3 to 8%, for both analytes. These data indicate that the IPD-MWCNTs are highly stable, and its active sites cannot be easily fouled, as compared to the oxidised MWCNTs adsorbent. The IPD-MWCNTS adsorbent was able to achieve lower LODs for both CPF and IMA (i.e. 0.026 and 0.033 $\mu g.L^{-1}$), and their corresponding LOQs are 0.078 and 0.100 $\mu g.L^{-1}$. The IPD-MWCNTs were able to achieve higher recoveries for both analytes at low and high concentrations (as well as in real water samples), whereas PRP can only achieve better recoveries at high concentrations.

Acknowledgements Gratitude to the National Research Foundation for the financial support and Dr Jaime Wesley-Smith at Microscopy unit of Sefako Makgatho Health Sciences University.

Author contribution All authors contributed to the study formation and constructing. LS undertook the material preparation, analysis, and draft manuscript writing. Prof Magadzu and Prof Ambushe reviewed the initial draft manuscript and commented with suggestions. All authors read and approved the final manuscript.

Funding Open access funding provided by University of Limpopo. This work was funded by National Research Foundation (Thuthuka Grant No. 118122). The foundation did not play any role in study design, sample collection, analysis, data interpretation, writing of the manuscript, and the decision to submit the manuscript for publication.

Data availability The data used during the current study are not sensitive in nature and are available from the corresponding author on request.

Declarations

Conflict of interest The authors declare that there are no conflicts of interest with regard to the publication of this paper.

Ethical approval There is no ethical approval required.

References

Abdullah TA, Juzsakova T, Hafad SA, Rasgeed RT, Al-Jammal N, Mallah MA, Salman AD, Le PC, Domokos E, Aldulaimi M (2021) Functionalised MWCNTs for oil spill clean-up from water. Clean Tech Environ Policy. https://doi.org/10.1007/s10098-021-02104-0

Alotaibi MS, Almousa NH, Asaker MA, Alkasmoul FS, Khdary NH (2021) Morphological: optical and mechanical characterisation of non-activated and activated nanocomposites of SG and MWCNTs. Crystals 11(1280):1–16. https://doi.org/10.3390/cryst11111280

Alothman ZA, Wabaidur SA (2019) Application of carbon nanotubes in extraction and chromatographic analysis: a review. A J Chem 12:633–651. https://doi.org/10.1016/j.arabjc.2018.05.012

Alothman ZA, Badjah AY, Locatelli M, Ali I (2020) Multi-walled carbon nanotubes solid phase extraction and capillary electrophoresis methods for the analysis of 4-cyanophenol and 3-nitrophenol in water. Molecules 25:1–9. https://doi.org/10.3390/molecules25173893

Ambrus A, Szenczi-Cseh J, Doan VVN, Vasarheleyi A (2023) Evaluation of monitoring data in foods. Agrochem 2:69–95. https://doi.org/10.3390/agrochemicals2010006

Atrache LLE, Hachani M, Kefi B (2016) Carbon nanotubes as solid-phase extraction sorbents for the extraction of carbamate insecticides from environmental waters. Int J Environ Sci Tech 13:201–208

Badawy MEI, Nouby MAM, Kimani PK, Lim LW, Rabea EI (2022) A review of the modern principles and applications of solid phase extraction techniques in chromatographic analysis. Anal Sci 38:1457–1487. https://doi.org/10.1007/s44211-022-00190-8

Bajorek A, Szostak B, Dulski M, Greneche JM, Lewinska S, Lizska B, Pawlyta M, Waniewska AS (2022) A comprehensive study of pristine and calcined f-MWCNTs functionalised by nitrogen-containing functional groups. Materials 15(977):1–21. https://doi.org/10.3390/ma15030977

Barbosa MO, Ribeiro RS, Ribeiro ARL, Pareira MFR, Silva AMT (2020) Solid-phase extraction cartridges with multi-walled carbon nanotubes and effect of the oxygen functionalities on the recovery efficiency of organic micropollutants. Sci Reports 10(22304):1–12. https://doi.org/10.1038/s41598-020-79244-8

Basivi PK, Ramesh S, Kakani V, Yadav HM, Bathula C, Afshar N, Sivasamy A, Kim HS, Pasupuleti VR, Lee H (2021) Ultrasonication-mediated nitrogen doped MWCNTs involving carboxyl methylcellulose composite for solid state supercapacitor application. Sci Reports 11:9918. https://doi.org/10.1038/s41598-021-89430-x

Bertrand PG (2019) Uses and misuses of agricultural pesticides in Africa: neglected public health threads for workers health and population. Intechopen. https://doi.org/10.5772/intechopen.84566

Cho G, Azzouzi S, Zucchi G, Lebental B (2022) Electrical and electrochemical sensors based on carbon nanotubes for the monitoring of chemicals in water: a review. Sens 22(218):1–59. https://doi.org/10.3390/s22010218

Chowdhry A, Kaur J, Khatri M, Puri V, Tuli R, Puri S (2019) Characterisation of functionalised multiwalled carbon nanotubes and comparison of their cellular toxicity between HEK 293 cells and zebra fish in vivo. Heliyon 5:1–11. https://doi.org/10.1016/j.heliyon.2019.e02605

Dhegihan M, Ansari M, Shahidi M, Kazemipour M (2021) Electrochemical fabrication of polypyrrole/hazelnut shells modified carbon nanocomposite sorbent for determination of polycyclic aromatic hydrocarbons using headspace solid-phase microextraction-gas chromatography. Green Chem Lett Rev 14(3):551–562. https://doi.org/10.1080/17518253.2021.1970243

Dubey R, Dutta D, Sarkar A, Chattopadhyay P (2021) Functionalised carbon nanotubes: Synthesis, properties, and applications in water purifications, drug delivery, and material and biomedical sciences. Nanoscale Adv 3:5722–5744. https://doi.org/10.1039/D1NA00293G

Espana PS, Miranda MM, Goti CL, Barrallo ES, Prados JLA (2022) Analysis of pesticide residues byQuEChERS method and LC-MS/MS for a new extrapolation of maximum residue levels in persimmon minor crop. Molecules 27(1517):1–16. https://doi.org/10.3390/molecules27051517

Freitas JF, Queiroz MELR, Oliveira AF, Ribeiro LP, Salvedor DV, Miranda LDL, Alves RR, Rodriguez AA (2023) Evaluation of imazalil dissipation/migration in post-harvest papaya using low temperature partition extraction and GC-MS analysis. Food Chem. https://doi.org/10.1016/j.foodchem.2023.135969

Gholami S, Llacuna JL, Vatampour V, Dehqan A, Paziresh S, Cortina JL (2022) Impact of a new functionalisation of multiwalled carbon nanotubes on antifouling and permeability of PVDF nanocomposite membranes for dye waste water treatment. Chemosphere 294(133699):1–12. https://doi.org/10.1016/j.chemosphere.2022.133699

Grinberg P, Methven BAJ, Swider K, Mester Z (2021) Determination of metallic impurities in carbon nanotubes by glow discharge mass spectrometry. ACS Omega 6:22717–22725. https://doi.org/10.1021/acsomega.1c03013

Gulati A, Mandeep MJ, Kakkar R (2020) Mesoporous rGO@ZnO composite: facile synthesis and excellent water treatment performance by pesticide adsorption and catalytic oxidative dye degradation. Chem Eng r Des 160:254–263. https://doi.org/10.1016/j.cherd.2020.04.040

Guo Y, Zhang J, Xu J, Wu X, Dong F, Liu X, Zheng Y (2021) An integrated strategy for purification by combining solid phase extraction with dispersive solid phase extraction for detecting 22 pesticides and metabolite residues in fish. J Agric Food Chem 69(25):7199–7208. https://doi.org/10.1021/acs.jafc.0c08040

Hoa LTM (2021) Surface functionalisation of MWCNTs with tris-(2-aminoethyl) amine and their characterisation. Adv Nat Sci Nanosci Nanotechnol 12:025014. https://doi.org/10.1088/2043-6262/abffca

Huq S (2011) A simple approach to automated SPE with Strata-X polymeric sorbents, Phenomenex: https://az621941.vo.msecnd.net/documents/3ad50824-f7f9-40ee-9863-0617659e2f47

Jajuli MN, Herzog G, Hebrant M, Poh NE, Rahim AA, Saad B, Hussin MH (2021) Graphene and zeolites as adsorbents in bar-micro-solid phase extraction of pharmaceutical compounds of diverse polarities. RSC Adv 11:16297–16306. https://doi.org/10.1039/D1RA01569A

Kashyap A, Singh NP, Arora S, Singh V, Gupta VK (2020) Effects of amino-functionalisation of MWCNTs on the mechanical and thermal properties of MWCNTs/epoxy composites. Bull Mater Sci 43:1–9. https://doi.org/10.1007/s12034-019-2012-0

Kim TH, Nam DH, Kim DH, Leem G, Lee S (2022) Fabrication of multi-vacancy-defect MWCNTs by the removal of metal oxide nanocomposites. Polymers 14:1–13. https://doi.org/10.3390/polym14142942

Kodali J, Talasila S, Arunraj B, Nagarathnam R (2021) Activated coconut charcoal as a super adsorbent for the removal of organophosphorus pesticide monocrotophos from water. Case Stud Chem Environ Eng 3:100099. https://doi.org/10.1016/j.cscee.2021.100099

Kumric K, Vujasin R, Egeric M, Petrovic D, Devecerski A, Matovic L (2019) Coconut shell activated carbon as solid phase extraction adsorbent for preconcentration of selected pesticides from water samples. Water Air Soil Pollut 230(302):1–10. https://doi.org/10.1007/s11270-019-4359-7

Ma J, Hou L, Wu G, Wang L, Wang X, Chen L (2020) Multiwalled carbon nanotubes for magnetic solid phase extraction of six heterocyclic pesticides in environmental water followed by HPLC-DAD determination. MDPI Mater 13(5729):1–14. https://doi.org/10.3390/ma13245729

Maranata GS, Surya NO, Hasanah AN (2021) Optimising factors affecting solid phase extraction performances of molecular imprinted polymer as recent sample preparation technique. Heliyon 7:1–10. https://doi.org/10.1016/j.heliyon.2021.e05934

Mas LI, Aparicio VC, De Geronimo E, Costa JL (2020) Pesticides in water sources used for human consumption in the semarid region of Argentina. SN Appl Sci. https://doi.org/10.1007/s42452-020-2513-x

Massoumi B, Razaei RM, Abbasian M, Jaymand M (2019) Amine-functionalised carbon nanotubes as curing agent for polystyrene-modified novolac epoxy resin: synthesis, characterisation and possible applications. Appl Phys A 304:1–7. https://doi.org/10.1007/s00339-019-2599-4

Mkhondo NB, Magadzu T (2014) Effects of different acid-treatment on the nanostructure and performance of carbon nanotubes in electrochemical hydrogen storage. Dig J Nanomat Biostr 9:1331–1338

Nawarathne CP, Hoque A, Ruhunage CK, Rahm CE, Alvarez NT (2021) Chemical bond formation between vertically aligned carbon nanotubes and metal substrates at low temperatures. Appl Sci 11(9529):1–15. https://doi.org/10.3390/app11209529

Nawaz N, Shad MA, Rehman N, Andaleeb H, Ullah N (2020) Effect of solvent polarity on extraction yield and antioxidant properties of phytochemicals from bean *(Phaseolus vulgaris)* seeds. Brazil J Pharma Sci 56:1–9. https://doi.org/10.1590/s2175-97902019000417129

Patel KK, Purohit R, Hashmi SAR, Gupta RK (2020) Effects of the diameter of MWCNTs on shape memory and mechanical properties of polyurethane composites. J Polymer Res 27(29):1–7. https://doi.org/10.1007/s10965-019-2003-2

Piao Y, Tondare VN, Davis CS, Gorham JM, Petersen EJ, Gilman JW, Scott K, Vladar AE, Walker ARH (2021) Comparative study of multiwall carbon nanotube nanocomposites by Raman, SEM, and XPS measurement techniques. Comp Sci Tech 208:108753. https://doi.org/10.1016/j.compscitech.2021.108753

Plunkett A, Kroning K, Fiedler B (2019) Highly optimised nitrogen doped MWCNTs through in-depth parametric study using design of experiments. Nanomater 9(4):1–16. https://doi.org/10.3390/nano9040643

Rao TN, Gaikwad S, Naidu TM, Han S (2020) Extraction and determination of pesticides in water using carbon nanotubes coupled with gas chromatography-mass spectroscopy. Kor J Chem Eng 27:1042–1049. https://doi.org/10.1007/s11814-020-0511-8

Risoluti R, Gullifa G, Carcassi E, Masotti A, Materazzi S (2020) TGA/Chemometrics addressing innovative preparation strategies for functionalised carbon nanotubes. J Pharma Analysis 10:351–355. https://doi.org/10.1016/j.jpha.2020.02.009

Rodriguez C, Leiva E (2020) Enhanced heavy metal removal from acid mine drainage wastewater using double-oxidised MWCNTs. Molecules 25(1):1–22. https://doi.org/10.3390/molecules25010111

Sabri FNAM, Zakaria MR, Akil HM (2019) Dispersion and stability of multiwalled carbon nanotubes (MWCNTs) in different solvents. AIP Conf Proc Doi 10(1063/5):0024711

Sadegh H, Ali GAM, Agarwal S, Gupta VK (2019) Surface modification of MWCNTs with carboxylic acids to amine and their superb Adsorption performance. Int J Environ R 13:1–10. https://doi.org/10.1007/s41742-019-00193-w

Saidi NM, Norizan MN, Abdulla N, Janudin N, Kasim NAM, Osman MJ, Mohamed IS (2022) Charactarisations of MWCNTs nanofluids on the effects of surface oxidative treatments. Nanomater 12:1–26. https://doi.org/10.3390/nano12071071

Salah LS, Ouslimani N, Bousba D, Huynen I, Danlee Y, Aksas H (2021) Carbon nanotubes (CNTs) from synthesis to functionalised CNTs using conventional and new chemical approaches. J Nanomater. https://doi.org/10.1155/2021/4972770

SANTE/11945/2015 guidance document on analytical. No. 10509. APPLICATION NOTE

Schwantes D, Goncalves AC, Conradi E, Campacnolo MA, Zimmermann J (2020) Determination of chlopyrifos by GC/ECD in water and its sorption mechanism study in a RHODIC FERRALSOL. J Environ Health Sci Eng 18(10):149–162.

Scigalski P, Kosobucki P (2020) Recent materials developed for dispersive solid phase extraction. Molecules 25(4869):1–26. https://doi.org/10.3390/molecules25214869

Selambakkannu S, Othman NAF, Bakar KA, Karim ZA (2019) Adsorption studies of packed column for the removal of dyes using amine functionalised radiation induced grafted fibre. SN Appl Sci 1:175. https://doi.org/10.1007/s42452-019-0184-2

Semiz A, Duman O, Tunc S (2020) Development of a reversed phase-high performance liquid chromatographic method for the analysis of glucosamine sulphate in dietary supplement tablets. J Food Compos Anal 93:103607. https://doi.org/10.1016/j.jfca.2020.103607

Sezer N, Koc M (2019) Oxidative acid treatment of carbon nanotubes. Surf Inetrf 14:1–8. https://doi.org/10.1016/j.surfin.2018.11.001

Shah R (2020) Pesticides and human health. Emerg Contam. https://doi.org/10.5772/intechopen.93806

Sibaja SBB, Ramirez DP, Huerta AMT, Crespo MAD, Rosales HJD, Salaraz AER, Meneses ER (2021) CVD conditions for MWCNTs production and their effects on the optical and electrical properties of PPy/MWCNTs, PANI/MWCNTs nanocomposites by in situ electropolymerization. Polym (basel) 13(351):1–59. https://doi.org/10.3390/polym13030351

Silva WM, Ribeiro H, Seara LM, Clado HDR, Ferlauto AS, Paniago RM, Leite CF, Silva GG (2012) Surface properties of oxidised and aminated MWCNTs. J Braz Chem Soc 6:1078–1086. https://doi.org/10.1590/S0103-50532012000600012

Soheilifard F, Marzban A, Raini MG, Taki M, Zelm R (2020) Chemical footprint of pesticides used in citrus orchards based on canopy deposition and off-target losses. Sci Tot Environ 732(139118):1–11. https://doi.org/10.1016/j.scitotenv.2020.139118

Speltini A, Profumo A, Merli D, Grossi N, Milanese C, Dondi D (2019) Tuning retention and selectivity in reversed-phase liquid chromatography by using functionalised multiwalled carbon nanotubes. Arab J Chem 12:541–548. https://doi.org/10.1016/j.arabjc.2015.05.016

Sreejarani K, Ramontja J, Ray SS (2011) Amine functionalisation of carbon nanotubes for the preparation of CNT based polyactide composite – a comparative study. ACS 22:1–16

Su HC, Lin AY (2003) High performance liquid chromatographic determination of imazalil in agriculturalproducts. J Food and Drug Anal 11(4):296–301

Sun L, Yuan G, Gao L, Yang J, Chhowalla M, Gharahcheshmeh MH, Gleason KK, Choi YS, Hong BH, Liu Z (2021) Chemical vapor deposition. Nat Rev Methods Primers. https://doi.org/10.1038/s43586-020-00005-y

Syafrudin M, Kristanti RA, Yuniarto A, Hadibarata T, Rhee J, Al-onazi WA, Algarni TS, Almarri AH, AL-Mohaimeed AM, (2021) Pesticides in drinking water- a review. Int J Environ Res Public Health 18(468):1–15.

Tankiewicz M (2019) Determination of selected priority pesticides in high water fruits and vegetables by modified QuEChERS and GC-ECD with GC-MS/MS confirmation. Molecules 24:417. https://doi.org/10.3390/molecules24030417

Thi L, Hoa M (2021) Surface functionalisation of MWCNTs with Tris(2-aminoehtyl)amine and their characterisation. Adv Nat Sci: Nanosci Nanotech 12:1–9. https://doi.org/10.1088/2043-6262/abffca

Trapani M, Mazzaglia A, Piperno A, Cordaro A, Zagami R, Castriciano MA, Romeo A, Scoalro MM (2020) Novel nanohybrids based on supramolecular assemblies of meso-tatrakis-(4-sulfonatophenyl) porphyrin J-aggregates and amine functionalised carbon nanotubes. Nanomater 10(669):1–14. https://doi.org/10.3390/nano10040669

Tserengombo B, Jeong H, Dolgor E, Delgado A, Kim S (2021) Effect of functionalisation in different conditions and ball milling on the dispersion and thermal and electrical conductivity of MWCNTs in aqueous solution. MDPI Nanomater 11:1–12

Veloo KV, Ibrahim NAS (2021) Analytical extraction methods and sorbents development for simultaneous determination of organophosphorus pesticides residues in food and water samples: a review. Molecules 26(5495):1–20. https://doi.org/10.3390/molecules26185495

Wang B, Pang B (2020) The Influence of *N,* N-dimethylformamide on dispersion of multiwalled carbon nanotubes. Russ J Phys Chem 94(4):810–817. https://doi.org/10.1134/S0036024420040019

Wang S, Li M, Li X, Li S, Zhang Q, Li H (2020) A functionalised carbon nanotube nanohybrids-based QuEChERS method for detection of pesticide residues in vegetables and fruits. J Chrom A 1631(461526):1–11. https://doi.org/10.1016/j.chroma.2020.461526

Wang J, Duan HL, Fan L, Lin YM, Sun JN, Zhang ZQ (2021a) Magnetic tetraethylenepentamine modified multiwalled carbon nanotubes as clean-up materials for organophosphorus pesticide residues analysis in cucumber. F Contr 124:107904. https://doi.org/10.1016/j.foodcont.2021.107904

Wang Z, Xu W, Jie F, Zhao Z, Zhou K, Liu H (2021b) The selective adsorption performance and mechanism of multiwall magnetic carbon nanotubes for heavy metals in wastewater. Sci Reports 11(16878):1–13. https://doi.org/10.1038/s41598-021-96465-7

Wang Y, Tian J, Wang Z, Li C, Li X (2022) Crop-safe pyraclostrobin-loaded mutliwalled carbon nanotube delivery systems: Higher fungicidal activity and lower acute toxicity. Agric Sci Tech 2:534–545. https://doi.org/10.1021/acsagscitech.1c00293